Mild air oxidation of boron nitride nanotubes. Application as nanofillers for thermally conductive polycarbonate nanocomposites.

Antoine Bodin, Thomas Pietri, Jean-Pierre Simonato

Mild air oxidation of boron nitride nanotubes. Application as nanofillers for thermally conductive polycarbonate nanocomposites.

Antoine Bodin, Thomas Pietri, Jean-Pierre Simonato

Nanotechnology

Mild air oxidation of boron nitride nanotubes. Application as nanofillers for thermally conductive polycarbonate nanocomposites

To cite this article before publication: Antoine Bodin *et al* 2022 *Nanotechnology* in press https://doi.org/10.1088/1361-6528/acae2b

Mild Air Oxidation of Boron Nitride Nanotubes. Application as Nanofillers for Thermally Conductive Polycarbonate Nanocomposites.

Antoine Bodin [§], *Thomas Pietri* [§] *and Jean-Pierre Simonato* [§]*

[§] University Grenoble Alpes, CEA, LITEN, DTNM, F-38000 Grenoble, France

E-mail: jean-pierre.simonato@cea.fr

* Corresponding author

KEYWORDS: Boron nitride nanotubes, air oxidation, NHPI, catalysis, nanocomposites.

ABSTRACT

Boron nitride nanotubes (BNNTs) have experienced considerable growth in recent years due to their unique intrinsic properties, in particular for the fabrication of polymer nanocomposites. Dispersion of pure BNNTs in nanocomposites is often difficult due to their poor compatibility with most polymer matrices. An approach involving the creation of hydroxyl groups on their surface could improve their dispersion. While some harsh oxidation processes have been reported so far, a mild oxidation of BNNTs using air as the oxidant is reported here. This new catalytic reaction leads to slightly oxidized BNNTs, which were characterized by SEM, XPS, FTIR and TGA. Polycarbonate nanocomposites were then fabricated using pristine and oxidized BNNTs as nanofillers. The measured thermal conductivity increased linearly with the mildly oxidized BNNTs content. It reached a five-fold increase up to 1.19 W/m.K at 15% vol. content which is significantly improved over nanocomposites fabricated with severely oxidized BNNTs, while the electrically insulating character remained unchanged.

1. INTRODUCTION

Boron nitride-based nanomaterials are continuously drawing interest from the scientific community [1,2]. They are used in a variety of applications and especially in cases where heat dissipation is of primary consideration [3,4]. Among these boron nitride-based nanomaterials, two nanostructures have attracted particular attention for applications as nanofillers in polymer nanocomposites: boron nitride nanosheets (BNNS, 2D) and boron nitride nanotubes (BNNTs, 1D). Although BNNS have been of great interest in the development of thermally conductive polymer nanocomposites [5–7], this paper focuses specifically on BNNTs. With recent development [8,9], BNNTs are now emerging as very promising 1D nanofillers for heat dissipation applications [10–12]. They are geometrically very close to carbon nanotubes (CNTs) except that the carbon-carbon bonds are replaced by alternating boron-nitrogen bonds. While they possess very good thermal conductivity and mechanical properties comparable to those of CNTs, BNNTs are electrically insulating (band gap > 5.5 eV) and thermally stable up to 1000 °C under air [13,14].

For many applications in nanocomposites, the pristine form of the BNNTs is not fully satisfactory due to insufficient stabilizing interactions with the polymer matrices. This often leads to poor dispersion resulting in the formation of BNNTs bundles in the polymer matrix. Although BNNTs are practically chemically inert ant quite resistant to oxidation [15], several approaches involving chemical functionalization of the nanotubes have been developed to improve their dispersion [16–21]. It should be mentioned that much effort has also been devoted to the functionalization of boron nitride nanosheets (BNNS), the 2D counterpart of BNNTs [22–25]. The first step of BNNT functionalization is commonly based on the oxidation of the nanotubes to activate the surface, followed by various reactions with molecules of interest. Different functionalization routes using hydroxylated BNNTs have been reported to be effective in

providing greater solubility or dispersion of the nanotubes through stabilizing interactions [26–30].

One of the main difficulties of the reported oxidation processes is to reach a sufficient level of oxidation on the surface of the nanotubes to ensure a good density of hydroxyl groups, without being too harsh to avoid over-oxidation. Indeed, Liao et al. [31] showed that over-oxidation related to severe reaction conditions leads to the nanostructure destruction (removed end-caps, sharpened ends, thinned sidewalls and shortened lengths), resulting in a loss of the remarkable properties. Since the intrinsic chemical reactivity of BNNTs is quite low, only a few oxidation routes have been successfully tested so far, especially under harsh conditions. Such severe oxidation protocols include the use of nitric acid [27,30,32], perchloric acid [26], concentrated sodium hydroxide solution [28,33], excess bromine in water [34–37] or hydrogen peroxide under pressure [38,39]. A fine control of the nanotube oxidation is somewhat difficult due to these harsh conditions. It should also be noted that gas-phase oxidation of BNNTs exists [40–43].

Among various oxidation reactions used in organic chemistry, a catalytic free-radical reaction based on N-Hydroxyphthalimide (NHPI) has been widely developed for the air oxidation of organic molecules such as alkanes, alcohols or aldehydes [44–46]. This oxidation reaction is known to give better conversion and selectivity than conventional autoxidations [47]. A main advantage of this system relies on the use of air as the final oxidant of the reaction. To the best of our knowledge, this catalytic system has never been used for oxidizing inorganic compounds. In most cases, the oxidation reaction of BNNTs occurs through a concerted mechanism [27,34]. However, some recent reports revealed that BNNTs could undergo surface activation through free-radical reactions [48,49]. Shin et al. [48] predicted via theoretical study and experimentally verified the functionalization of pristine BNNTs using chemically reduced nanotubes with sodium

naphthalide followed by reactions with free radicals. Lin et al. [49] used thermally labile peroxides to covalently functionalize BNNTs. Upon heating, the peroxides decompose to generate radicals that are capable of reacting with the BNNTs.

In this article, it is demonstrated that such a catalytic system based on NHPI efficiently catalyses the air oxidation of BNNT and affords a straightforward route to the fabrication of mildly oxidized BNNTs.

The advantages of using mild over harsh oxidation conditions and the effects of such oxidation protocols on thermal properties of polymer nanocomposites are also highlighted. The BNNTs were used as nanofillers dispersed in a polycarbonate matrix. Contrary to what had been reported with nanotubes oxidized according to the usual protocols [37], the moderately oxidized BNNTs behave like raw BNNTs, i.e. they allow a strong increase of the thermal conductivity (500% increase at 15 vol%) while maintaining a marked electrically insulating character.

2. EXPERIMENTAL SECTION

2.1 Materials

N-hydroxyphthalimide (NHPI, 97%), manganese(II) acetate ($Mn(OAc)_2$, 98%), cobalt(II) acetate ($Co(OAc)_2$, 99.9%), acetic acid (AcOH, glacial), sodium hydroxide (NaOH) and tetrahydrofuran (THF, 99.9%) were purchased from Sigma-Aldrich (USA) and used as received. Nitric acid (HNO_3, 69.5%) was purchased from Carlo Erba (Germany). Boron nitride nanotubes (BNNTs) were purchased from BNNano (USA) as Nanobar™ (purity = 90%, diameter ≈ 250-300 nm / length ≈ 20 µm) and used as received without any purification treatment. Polycarbonate (PC, grade Makrolon LED2045) was purchased from Covestro (Germany).

2.2. Experiments

2.2.1. Oxidation of BNNT

BNNTs were oxidized into BNNT-OH through a catalytic reaction based on NHPI and transition metals such as manganese and cobalt. In a typical experiment, 200 mg of pristine BNNTs were firstly dispersed in 150 mL of glacial acetic acid for 30 min in an ultrasonic bath. Simultaneously, 260 mg (20 mol%) of NHPI, 7 mg (0.5 mol%) of $Mn(OAc)_2$ and 7 mg (0.5 mol%) of $Co(OAc)_2$ were dispersed in 50 mL of glacial acetic acid for 30 min. Once fully dispersed, the BNNTs solution and the [NHPI + $Mn(OAc)_2$ + $Co(OAc)_2$] solution in glacial acetic acid were put together and placed under a reflux heating set at 100 °C with magnetic stirring and controlled air bubbling. The reaction mixture was left under these conditions for 64 h. The resulting hydroxylated BNNTs (BNNT-OH|*[NHPI]*) were finally vacuum-filtered and washed four times with 200 mL of

deionized water to remove catalysts and residual NHPI. The purified BNNT-OH|*[NHPI]* powder was then dried in an oven set at 80°C for several hours before any further experiment.

For comparison purposes, pristine BNNTs were also treated with concentrated nitric acid (HNO_3 69.5%) for 3 h in an ultrasonic bath (BNNT-OH|*[HNO_3]*) and concentrated sodium hydroxide aqueous solution (NaOH 10 M) for 20 h at 100 °C (BNNT-OH|*[NaOH]*).

2.2.2. Nanocomposite preparation

PC-BNNT and PC-BNNT-OH nanocomposites were synthesized through the solution mixing technique. Briefly, PC was firstly dissolved in THF (1 h stirring at room temperature) and simultaneously, BNNTs or BNNT-OH were dispersed in THF at a concentration of 1 mg/mL (10 min stirring at room temperature followed by 10 min in an ultrasonic bath). Then, the BNNTs/THF or BNNT-OH/THF solution was incorporated into the PC/THF solution and stirred for 30 min. Finally, the excess of THF was removed using a rotary evaporator. The resulting dry nanocomposite flakes were left one night under a fume hood for an additional drying.

PC-BNNT and PC-BNNT-OH nanocomposite flakes were then used to produce bulk samples (disk-shaped, diameter = 13 mm, thickness = 1.2 mm). The disk-shaped samples were obtained by hot pressing the nanocomposite flakes under a uniaxial hot press set at 270 °C (Carver 30T 4128, Carver Inc., USA). Prior to molding, the nanocomposite flakes were dried in an oven set at 120 °C for at least 3 h. Then, the nanocomposite flakes were put inside a pressing die and preheated 20 min at 270 °C. Finally, a 5 min pressing at 270 °C of the nanocomposite flakes resulted in the desired disk-shaped sample. The pressing die was then cooled down to room temperature. Different nanofiller weight fractions (wt%) were investigated in this study. For comparison purposes, they were also converted into volume fractions (vol%) using the following formula:

$$vol\% = \frac{wt\%}{wt\% + \left(\frac{\rho_f}{\rho_m}\right) * (1 - wt\%)}$$

where ρ_f is the density of the filler (ρ_{BNNT} = 2.3 g cm^{-3}) and ρ_m is the density of the polycarbonate matrix (ρ_{PC} = 1.2 g cm^{-3}).

2.3. Characterizations

The morphology of BNNTs and BNNT-OH was observed using a field-emission - scanning electron microscope (FE-SEM, LEO 1530 VP Gemini, Zeiss, Germany). Diameters and lengths of BNNTs and BNNT-OH were measured using the digital image processing software ImageJ. The dispersion of BNNTs and BNNT-OH inside the polycarbonate matrix was also studied by FE-SEM coupled with energy dispersive X-ray spectroscopy (EDX, XFlash Detector 5030, Bruker, Germany) on bulk nanocomposites fracture surfaces. Before any observation, all samples were metalized by platinum sputtering.

Infrared spectra of BNNTs and BNNT-OH samples were obtained with a Fourier transform infrared (FTIR) apparatus used in transmission mode (Vertex 70, Bruker Optics, Germany). In a typical analysis, a spatula tip amount of BNNTs or BNNT-OH powder was mixed with KBr grinded crystals and disk-shaped under a uniaxial hydraulic press. All KBr samples were dried in an oven set at 80 °C before any FTIR analysis to avoid water contamination.

X-ray photoelectron spectra of BNNTs and BNNT-OH were obtained with a X-ray photoelectron spectroscopy (XPS) apparatus (Versaprobe-II, Physical Electronics, USA).

Mass loss percentage with increasing temperature was measured by thermogravimetric analysis (TGA) using a STA 449 from Netzsch, Germany. Two measurements were carried out for each material. A heating rate of 5 °C/min up to 600 °C was applied under air atmosphere.

Thermal conductivity values (λ) were calculated using the formula $\lambda = \alpha * \rho * C_p$, where α is the measured thermal diffusivity, ρ is the measured bulk density and C_p is the calculated heat capacity based on the rule of mixtures. Through-plane ($\perp$) and in-plane (//) thermal diffusivity measurements were performed using a laser flash apparatus at 25 °C (LFA447 MicroFlash, Netzsch, Germany). For in-plane measurements, the disk-shaped samples were cut into ≈1.2 mm-wide strips using a diamond-coated wire saw, rotated 90° and placed inside a square sample holder. Bulk density was measured in a 1 cm^3 cell with a He gas displacement pycnometry system at 25 °C (Accupyc II 1340 from Micromeritics, USA). The average value was calculated from 25 measurements.

Electrical resistivity was measured using a high resistivity measurement system mounted with a UR-SS probe (Hiresta-UX, MCP-HT800, Mitsubishi Chemical Analytech, Japan).

3. RESULTS AND DISCUSSION

3.1. Synthesis and characterization of oxidized BNNTs (BNNT-OH)

The objective of this study was to mildly oxidize BNNTs through a soft and straighhtforward method using air as the final oxidant. The oxidation reaction of BNNTs was carried out in a conventional benchtop setup, with a flow-regulated air bubbler placed in the solution, as displayed in figure 1.

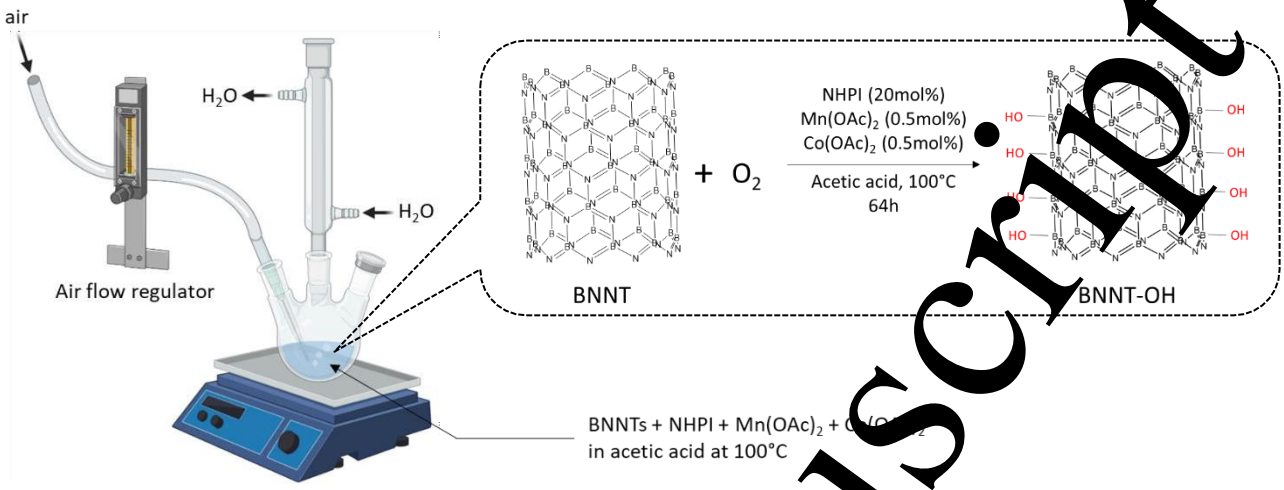

Figure 1. Schematic view of the catalytic air oxidation process of BNNTs

After reaction, the BNNT-OH were filtered, washed, dried and then analyzed by a set of characterization techniques. High-resolution SEM images of the nanotubes were compared before and after the oxidation reaction. They are displayed in figure 2. Although the BNNTs appeared slightly modified after the reaction with NHPI (slight modification of the nanotube diameter), their overall integrity was maintained (figure 2(a-b)). BNNTs entanglement made length measurements difficult, however it appears that BNNT-OH (figure 2(b)) were slightly shorter than pristine BNNTs (figure 2(a)). In contrast, BNNT-OH obtained after HNO_3 or NaOH based reactions underwent significant degradation as shown in figure 2(c-d). These degradations are typical of severe oxidation processes and include thinned sidewalls (drastic reduction of the nanotube diameter in BNNT-OH|*[HNO_3]* and BNNT-OH|*[NaOH]* samples), sharpened ends and tearing or breakage of nanotubes (figure 2(c)) [31]. SEM images of oxidized BNNTs are shown in figure S1.

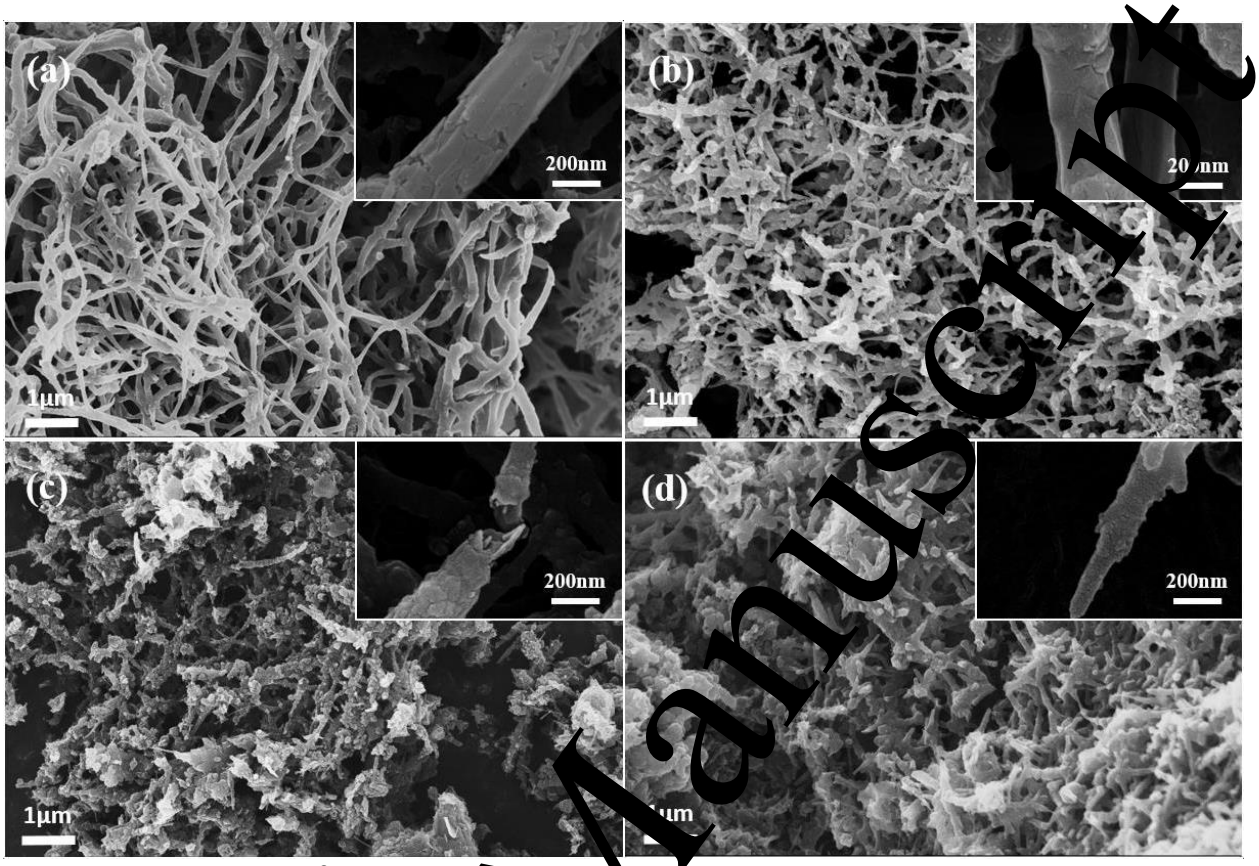

Figure 2. SEM images of (a) pristine BNNTs, (b) BNNT-OH|*[NHPI]*, (c) BNNT-OH|*[HNO_3]* and (d) BNNT-OH|*[NaOH]*. Insets show typical high magnification images of individual BNNTs.

Oxidized BNNTs were analyzed by FTIR. The full-scale FTIR spectra of pristine and oxidized BNNTs are displayed in figure 3(a). An inset of the 2800-4000 cm^{-1} region is also presented in figure 3(b). The IR spectrum of pristine BNNT is similar to previous reports in the literature [50,51]. Two major absorption bands are observed at 811 and 1380 cm^{-1} which are indicative of the out-of-plane B-N-B bending and the in-plane B-N stretching vibrations respectively. This is typical of hexagonal boron nitride with symmetries of A_{2u} and E_{1u} [52,53]. The comparison of the 2800-4000 cm^{-1} region between pristine BNNTs and BNNT-OH shows the appearance of a peak at 3435 cm^{-1}, which can be ascribed to the vibration frequency of the hydroxyl groups. The BNNT-OH|*[NHPI]* sample exhibits the highest relative absorbance intensity compared to BNNT-OH|*[HNO_3]* and BNNT-OH|*[NaOH]* (figure 3(b)).

The comparative XPS analysis of the pristine and oxidized BNNT reveals a slight but significant modification of the spectrum as displayed in figure 3(c-f). The peak around 190.3 eV was attributed to the B-N bond [39]. In pristine BNNTs (figure 3(c)), the B1s peak is symmetric with respect to its center located at 190.3 eV and well fitted with a single Gaussian component. On the contrary, for oxidized BNNTs (figure 3(d-f)), the B1s peak appears asymmetric with shoulders at higher binding energies. After peak deconvolution, the presence of a second Gaussian component centered at 191.3 eV in BNNT-OH|*[NHPI]* and BNNT-OH|*[HNO_3]* samples can be assigned to the B-O bond [38,39,54] thus confirming the surface oxidation of BNNTs. Interestingly, the B1s peak in the BNNT-OH|*[NaOH]* sample (figure 3(f)) display less asymmetry, suggesting a lower hydroxyl density after functionalization.

TGA experiments were also carried out to confirm the presence of -OH groups after the oxidation reaction. TGA curves of pristine and oxidized BNNTs are presented in figure S2. While pristine BNNTs remained thermally stable over the entire temperature range (no noticeable mass loss), BNNT-OH underwent a slight mass loss between 250 and 450°C. This mass loss corresponds to the elimination of the hydroxyl groups (de-hydroxylation) [30,55], confirming the presence of -OH groups at the surface of BNNTs after oxidation. However, it should be noted that the mass loss is slightly different depending on the oxidation process employed. The most important mass loss (about 0.77%) is obtained with the BNNT-OH|*[NHPI]* sample, which is consistent with both FTIR and XPS characterization results.

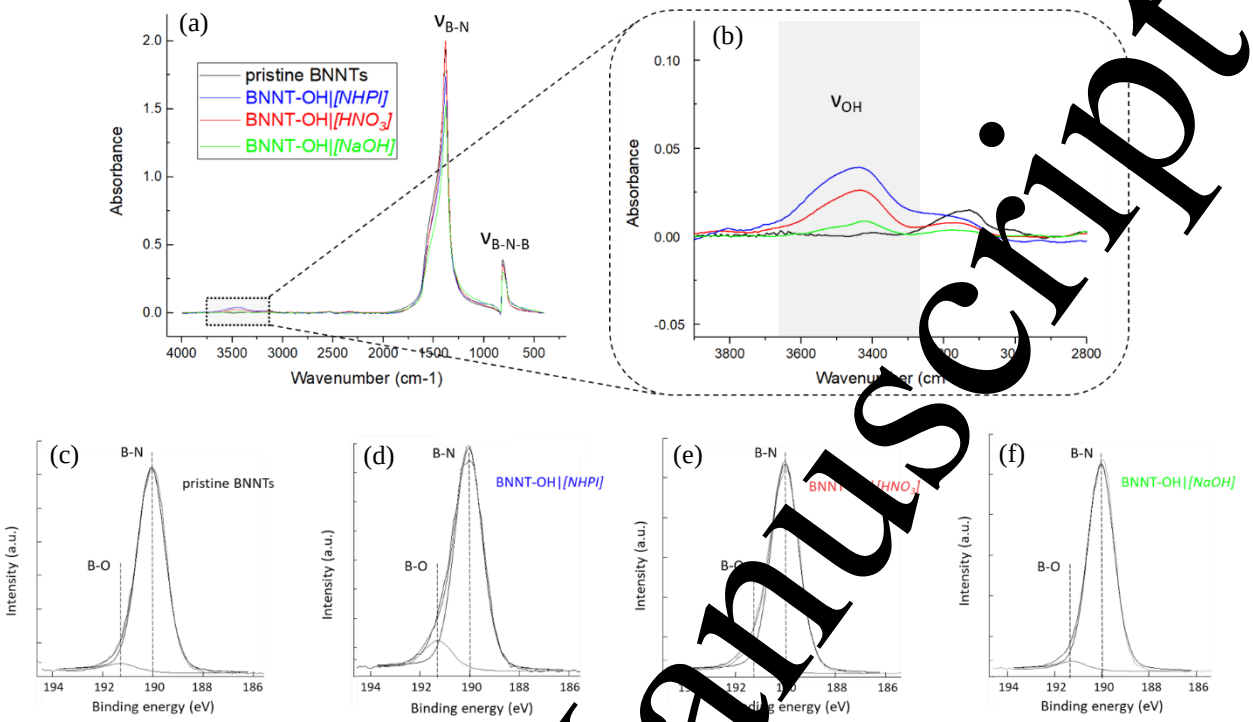

Figure 3. (a) FTIR spectra of pristine and oxidized BNNTs, (b) zoom of the FTIR spectra in the 2800-4000 cm^{-1} range. Narrow B1s scans of high resolution XPS spectra of (c) pristine BNNTs and (d-f) oxidized BNNTs.

3.2. Thermally conductive nanocomposites

Nanocomposites were prepared using polycarbonate (PC) as the polymer matrix. PC is a high-performance and heat-resistant thermoplastic polymer with very good mechanical properties and dimensional stability even at high temperatures. PC nanocomposites with various nanofiller loadings were carried out through the solution mixing technique. The thermal conductivity measurements of nanocomposites prepared with pristine and oxidized BNNTs are plotted in figure 4(a). A blank experiment realized without BNNTs confirmed the expected thermal conductivity of PC at 0.21-0.23 W/m.K [56]. The reference material was chosen as the pure PC loaded with unmodified BNNTs (black data points in figure 4(a)). The thermal conductivity of the PC-BNNTs nanocomposites was found to increase linearly with the BNNT content with a maximum through-

plane value $\lambda_{\perp}$ = 0.87 W/m.K and in-plane value $\lambda_{//}$ = 1.08 W/m.K at 15% vol. content. This corresponds to more than a four-fold increase compared to the pristine polymer, showing that BNNTs are very efficient nanofillers for increasing the heat dissipation capacity of the polymer. Regarding oxidized BNNTs, the thermal conductivity values measured on PC-BNNT-OH|*[HNO_3]* and PC-BNNT-OH|*[NaOH]* nanocomposites are clearly worsened. These results obtained with pristine BNNTs and BNNTs treated under harsh conditions (BNNT-OH|*[HNO_3]* and BNNT-OH|*[NaOH]*) are fully consistent with the recent report of Zandieh et al. [37]. In this study, the authors found similar results on the thermal conductivity on PC nanocomposites filled with pristine BNNTs and BNNTs oxidized with excess bromine in water, which is equally considered as a harsh oxidizer. Interestingly, the BNNTs treated with our protocol based on the NHPI catalytic oxidation did not alter the thermal conductivity of the PC nanocomposite (blue data points in figure 4(a)), they even slightly improved the in-plane thermal conductivity with a value of $\lambda_{//}$ = 1.19 W/mK at 15% vol. content. At high filler loadings, the in-plane thermal conductivity of PC-BNNT-OH|*[NHPI]* was clearly higher than the one of PC-BNNTs (figure 4(b)), suggesting a better phonon diffusion throughout the whole nanocomposite. The difference between through-plane and in-plane thermal conductivity results observed in figure 4(a-b) can be ascribed to a partial alignment of the BNNTs perpendicularly to the pressing direction during the disk-shaping process, favoring a phonon transport in the in-plane direction [57–59]. SEM images and EDX mappings of fracture surfaces of pristine PC and PC nanocomposites filled with BNNT-OH fillers are presented in figure S3(a-b). The EDX mapping images suggest a better dispersion of hydroxylated BNNTs within the PC matrix compared to pristine BNNTs which tend to form large agglomerates (figure S2(a)). However, no significant difference was observed regarding the quality of the filler/matrix interface in the different samples with BNNT-OH as nanofillers (figure S3(b)). The lower thermal

conductivity recorded for nanocomposites using BNNTs oxidized under harsh conditions (HNO_3, NaOH, Br_2/H_2O) can thus be ascribed to the creation of large defects inside the BNNTs structure (figure 4(c)), as observed in figure 2 and figure S1. As surface hydroxylation implies the cleavage of several B-N bonds, the damaging of the h-BN lattice certainly induces significant loss of the nanomaterial properties, thus amplifying the phonon-defect scattering which results in a decrease of the overall thermal conductivity. The results obtained with BNNTs treated under mild conditions (BNNT-OH|*[NHPI]*), suggest a controlled oxidation rate, with less defects (figure 4(d)). The phonon-defect scattering is therefore minimized and the thermal conductivity of the nanocomposite not significantly altered. Electrical resistivity was also measured on the different nanocomposites. No significant change was observed with respect to the pure PC (figure 4(e)). It is consistent with the expected properties of BNNTs that are wide band gap insulators. This confirms the high potential of these nanofillers to fabricate nanocomposites being both thermally conductive and electrically insulating.

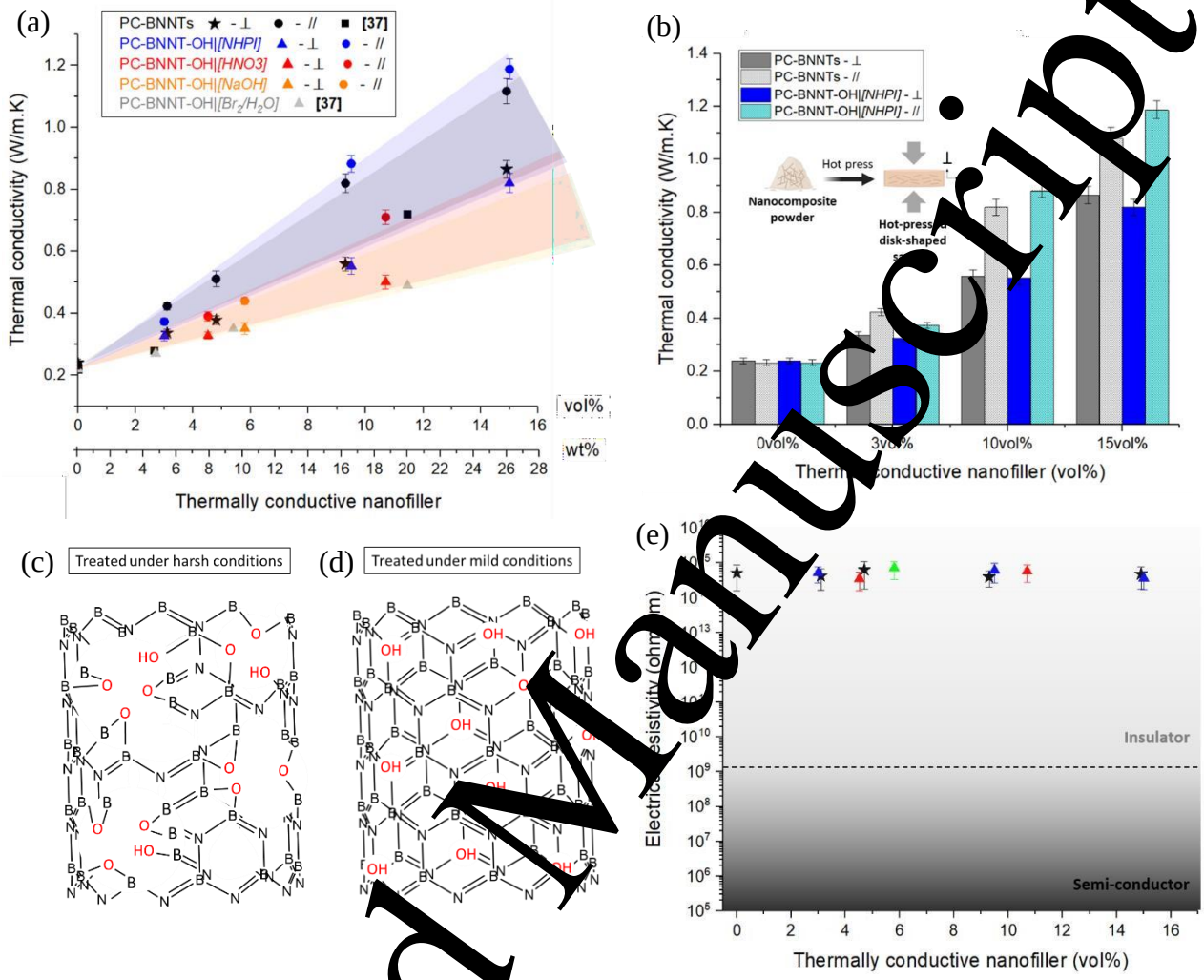

Figure 4. (a) In-plane and through-plane thermal conductivities of PC nanocomposites with pristine and oxidized BNNTs, (b) in-plane and through-plane thermal conductivities of PC-BNNTS vs PC-BNNT-OH[*NHPI*]. Schematic representation of oxidized BNNTs (c) under harsh and (d) under mild oxidizing conditions. (e) Electrical resistivity of PC nanocomposites filled with pristine and oxidized BNNTs.

4. CONCLUSION

In summary, three oxidation routes of pristine BNNTs have been tested including two severe oxidation protocols (concentrated HNO_3 and concentrated NaOH) and a new mild oxidation reaction. To our knowledge, the catalytic air oxidation of BNNTs is reported herein for the first time. All the oxidized BNNTs were characterized by a set of techniques demonstrating unambiguously the presence of hydroxyl groups on their surface. In contrast to the severely oxidized BNNTs, those oxidized by the NHPI route have largely retained their structural integrity. The oxidized BNNTs were used as nanofillers for the fabrication of nanocomposites with a PC matrix. Though severely oxidized BNNTs resulted in the degradation of the thermal conductivity of PC nanocomposites compared to the pristine ones, mildly oxidized BNNTs allowed a five-fold improvement of the thermal conductivity at 1.2% vol. content. Functionalization of the mildly oxidized BNNT prepared according to reported protocol appears as a promising way to further increase the dispersion within the matrix, without damaging the integrity of the nanotubes, and thus to enhance the performances of the nanocomposites.

ASSOCIATED CONTENT

Supporting Information

Figure S1: High-resolution SEM images of pristine BNNTs and BNNT-OH.

Figure S2: TGA curves of pristine and oxidized BNNTs.

Figure S3(a): SEM images and EDX mappings of fracture surfaces of PC nanocomposites for assessment of BNNTs dispersion.

Figure S3(b): SEM images of fracture surfaces of PC nanocomposites for assessment of filler/matrix interface quality.

NOTE

The authors declare no competing financial interest.

ACKNOWLEDGEMENTS

The authors acknowledge Anass Benayad for helping in the XPS experiments and analysis. This work was supported by the Agence de l'Innovation de Defense (AID) through a PhD grant to A. Bodin.

DATA AVAILABILITY STATEMENT

The data that support the findings of this study are available upon reasonable request from the authors.

REFERENCES

[1] Aparna A, Sethulekshmi A S, Jayan J S, Saritha A and Joseph K 2021 Recent Advances in Boron Nitride Based Hybrid Polymer Nanocomposites *Macromolecular Materials and Engineering* **306** 2100429

[2] Gonzalez-Ortiz D, Salameh C, Bechelany M and Miele P 2020 Nanostructured boron nitride–based materials: synthesis and applications *Materials Today Advances* **8** 100107

[3] Sharma V, Kagdada H L, Jha P K, Śpiewak P and Kurzydłowski K J 2020 Thermal transport properties of boron nitride based materials: A review *Renewable and Sustainable Energy Reviews* **120** 109622

[4] Mazumder M R H, Mathews L D, Mateti S, Salim N V, Parameswaranpillai J, Govindaraj P and Hameed N 2022 Boron nitride based polymer nanocomposites for heat dissipation and thermal management applications *Applied Materials Today* **29** 101672

[5] Meziani M J, Sheriff K, Parajuli P, Priego P, Bhattacharya S, Rao A M, Quimby J L, Qiao R, Wang P, Hwu S-J, Wang Z and Sun Y-P 2022 Advances in Studies of Boron Nitride Nanosheets and Nanocomposites for Thermal Transport and Related Applications *ChemPhysChem* **23** e202100645

[6] Wu M, Zhou Y, Zhang H and Liao W 2022 2D Boron Nitride Nanosheets for Smart Thermal Management and Advanced Dielectrics *Advanced Materials Interfaces* **9** 2200610

[7] Yang L, Wang L and Chen Y 2020 Solid-state shear milling method to prepare PA12/boron nitride thermal conductive composite powders and their selective laser sintering 3D-printing *Journal of Applied Polymer Science* **137** 48766

[8] Xu T, Zhang K, Cai Q, Wang N, Wu L, He Q, Wang H, Zhang Y, Xie Y, Yao Y and Chen Y 2022 Advances in synthesis and applications of boron nitride nanotubes: A review *Chemical Engineering Journal* **431** 134118

[9] Lee C H, Bhandari S, Tiwari B, Yapici N, Zhang D and Yap Y K 2016 Boron Nitride Nanotubes: Recent Advances in Their Synthesis, Functionalization, and Applications *Molecules* **21** 922

[10] Zhang D, Zhang S, Yapici N, Oakley R, Sharma S, Parashar V and Yap Y K 2021 Emerging Applications of Boron Nitride Nanotubes in Energy Harvesting, Electronics, and Biomedicine *ACS Omega* **6** 20722–8

[11] Pietri T, Wiley B J and Simonato J-P 2021 Boron Nitride Nanotubes for Heat Dissipation in Polycaprolactone Composites *ACS Appl. Nano Mater.* **4** 4774–80

[12] Zhi C, Bando Y, Terao T, Tang C, Kuwahara H and Golberg D 2009 Towards Thermoconductive, Electrically Insulating Polymeric Composites with Boron Nitride Nanotubes as Fillers *Advanced Functional Materials* **19** 1857–62

[13] Zhi C, Bando Y, Tang C and Golberg D 2010 Boron nitride nanotubes *Materials Science and Engineering: R: Reports* **70** 92–111

[14] Turhan E A, Pazarçeviren A E, Evis Z and Tezcaner A 2022 Properties and applications of boron nitride nanotubes *Nanotechnology* **33** 242001

[15] Chen Y, Zou J, Campbell S J and Le Caer G 2004 Boron nitride nanotubes: Pronounced resistance to oxidation *Appl. Phys. Lett.* **84** 2430–2

[16] Yu J, Chen Y and Cheng B M 2009 Dispersion of boron nitride nanotubes in aqueous solution with the help of ionic surfactants *Solid State Communications* **149** 763–6

[17] McWilliams A D S, Martínez-Jiménez C, Shumard K R, Pasquinelli M and Martí A A 2022 Dispersion and individualization of boron nitride nanotubes *Journal of Materials Research*

[18] Kim D, Ha S, Choi H K, Yu J and Kim Y A 2018 Chemical assembling of amine functionalized boron nitride nanotubes onto polymeric nanofiber film for improving their thermal conductivity *RSC Adv.* **8** 4426–33

[19] Chang M S, Jang M-S, Yang S, Yu J, Kim T, Kim S, Jeong H, Park C R and Jeong J W 2020 Electrostabilized homogeneous dispersion of boron nitride nanotubes in wide-range of solvents achieved by surface polarity modulation through pyridine attachment *Nano Res.* **13** 344–52

[20] Martinez-Rubi Y, Jakubek Z J, Kingston C T, Barnes M B, Kim K S, Cheng F, Couillard M, Kingston C and Simard B 2015 Self-Assembly and Visualization of Poly(3-hexyl-thiophene) Chain Alignment along Boron Nitride Nanotubes *J. Phys. Chem. C* **119** 26605–10

[21] Zhou S-J, Ma C-Y, Meng Y-F, Su H-F, Zhu Z, Deng S-L and Xie S-Y 2012 Activation of boron nitride nanotubes and their polymer composites for improving mechanical performance *Nanotechnology* **23** 055708

[22] Sainsbury T, Satti A, May J, Wang Z, McGovern I, Gun'ko Y K and Coleman J 2012 Oxygen Radical Functionalization of Boron Nitride Nanosheets *J. Am. Chem. Soc.* **134** 18758–71

[23] Wu N, Yang W, Li H, Che S, Gao C, Jiang B, Li Z, Xu C, Wang X and Li Y 2022 Amino acid functionalized boron nitride nanosheets towards enhanced thermal and mechanical performance of epoxy composite *Journal of Colloid and Interface Science* **619** 388–98

[24] Liu Z, Dichiara A, Li D, Mateti S, Liu J, Yan F, Barrow C J, Chen Y, Ariga K and Yang W 2021 Challenges and solutions in surface engineering and assembly of boron nitride nanosheets *Materials Today* **44** 194–210

[25] Jiang H, Cai Q, Mateti S, Yu Y, Zhi C and Chen Y 2021 Boron Nitride Nanosheet Dispersion at High Concentrations *ACS Appl. Mater. Interfaces* **13** 44751–9

[26] Smith K K, Redeker N D, Rios J C, Mecklenburg M H, Marcischak J C, Guenthner A J and Ghiassi K B 2019 Surface Modification and Functionalization of Boron Nitride Nanotubes via Condensation with Saturated and Unsaturated Alcohols for High Performance Polymer Composites *ACS Appl. Nano Mater.* **2** 4053–60

[27] Ciofani G, Genchi G G, Liakos I, Athanassiou A, Dinucci D, Chiellini F and Mattoli V 2012 A simple approach to covalent functionalization of boron nitride nanotubes *Journal of Colloid and Interface Science* **374** 308–14

[28] Zhang C, Huang R, Wang Y, Wu Z, Guo S, Zhang H, Li J, Huang C, Wang W and Li L 2018 Aminopropyltrimethoxysilane-functionalized boron nitride nanotube based epoxy nanocomposites with simultaneous high thermal conductivity and excellent electrical insulation *J. Mater. Chem. A* **6** 20663–8

[29] Huang X, Zhi C, Jiang P, Golberg D, Bando Y and Tanaka T 2013 Polyhedral Oligosilsesquioxane-Modified Boron Nitride Nanotube Based Epoxy Nanocomposites: An Ideal Dielectric Material with High Thermal Conductivity *Advanced Functional Materials* **23** 1824–31

[30] Díez-Pascual A M and Díez-Vicente A L 2016 PEGylated boron nitride nanotube-reinforced poly(propylene fumarate) nanocomposite biomaterials *RSC Advances* **6** 79507–19

[31] Liao Y, Chen Z, Connell J W, Fay C C, Park C, Kim J-W and Lin Y 2014 Chemical Sharpening, Shortening, and Unzipping of Boron Nitride Nanotubes *Advanced Functional Materials* **24** 4497–506

[32] Ferreira T H, Marino A, Rocca A, Liakos I, Nitti S, Athanassiou A, Mattoli V, Mazzolai B, de Sousa E M B and Ciofani G 2015 Folate-grafted boron nitride nanotubes: Possible exploitation in cancer therapy *International Journal of Pharmaceutics* **481** 56–63

[33] Sharma S, Setia P, Chandra R and Thakur N 2020 Experimental and molecular dynamics study of boron nitride nanotube-reinforced polymethyl methacrylate composites *Journal of Composite Materials* **54** 3–11

[34] Guan J, Kim K S, Jakubinek M B and Simard B 2018 pH-Switchable Water-Soluble Boron Nitride Nanotubes *ChemistrySelect* **3** 9308–12

[35] Guan J, Derdouri A, Ashrafi B, Benhalima A, Kim K S, Daroszewska M and Simard B 2019 Boron nitride nanotubes reinforced polycarbonate nanocomposites *Materials Today Communications* **20** 100586

[36] Quiles-Díaz S, Martínez-Rubí Y, Guan J, Kim K S, Couillard M, Salavagione H J, Gómez-Fatou M A and Simard B 2019 Enhanced Thermal Conductivity in Polymer Nanocomposites via Covalent Functionalization of Boron Nitride Nanotubes with Short Polyethylene Chains for Heat-Transfer Applications *ACS Applied Nano Materials* **2** 440–51

[37] Zandieh A, Izadi H, Hamidinejad M, Shin H, Shi S, Martinez-Rubi Y, Guan J, Cho H, Kim K S and Park C B 2022 Molecular engineering of the surface of boron nitride nanotubes for

manufacture of thermally conductive dielectric polymer composites *Applied Surface Science* **587** 152779

[38] Wang W, Li Z, Prestat E, Hashimoto T, Guan J, Kim K S, Kingston C T, Simard B and Young R J 2020 Reinforcement of Polymer-Based Nanocomposites by Thermally Conductive and Electrically Insulating Boron Nitride Nanotubes *ACS Appl. Nano Mater.* **3** 364–74

[39] Zhi C Y, Bando Y, Terao T, Tang C C, Kuwahara H and Golberg D 2008 Chemically Activated Boron Nitride Nanotubes *Chemistry – An Asian Journal* **4** 1536–40

[40] Torres-Castillo C S and Tavares J R 2022 Covalent functionalization of boron nitride nanotubes through photo-initiated chemical vapour deposition *The Canadian Journal of Chemical Engineering* **n/a**

[41] Dai X J, Chen Y, Chen Z, Lamb P R, Li L H, Plessis J du, McCulloch D G and Wang X 2011 Controlled surface modification of boron nitride nanotubes *Nanotechnology* **22** 245301

[42] Ikuno T, Sainsbury T, Okawa D, Fréchet J M J and Zettl A 2007 Amine-functionalized boron nitride nanotubes *Solid State Communications* **142** 643–6

[43] Jakubinek M B, Kim K S, Homenick C, Fodra C, Walker S and Simard B 2019 Assessment of boron nitride nanotube materials using X-ray photoelectron spectroscopy *Can. J. Chem.* **97** 457–64

[44] Ishii Y, Sakaguchi S and Obora Y 2010 Aerobic Oxidations and Related Reactions Catalyzed by N-Hydroxyphthalimide *Modern Oxidation Methods* (John Wiley & Sons, Ltd) pp 187–240

[45] Ishii Y and Sakaguchi S 1999 A new strategy for alkane oxidation with O2 using N-hydroxyphthalimide (NHPI) as a radical catalyst *Catalysis Surveys from Asia* **3** 27–35

[46] Yang G, Zheng L, Wu G, Lin X and Song M 2007 Manganese Dioxide and N-Hydroxyphthalimide. An Effective Catalytic System for Oxidation of Nitrotoluenes with Molecular Oxygen *Advanced Synthesis & Catalysis* **349** 2445–8

[47] Ishii Y and Sakaguchi S 2006 Recent progress in aerobic oxidation of hydrocarbons by N-hydroxyimides *Catalysis Today* **117** 105–13

[48] Shin H, Guan J, Zgierski M Z, Kim K S, Kingston C T and Simard B 2015 Covalent Functionalization of Boron Nitride Nanotubes via Reduction Chemistry *ACS Nano* **9** 12573–82

[49] Lin S, Ashrafi B, Laqua K, Kim K S and Simard B 2017 Covalent derivatization of boron nitride nanotubes with peroxides and their application in polycarbonate composites *New J. Chem.* **41** 7571–7

[50] Dong Z and Song Y 2010 Transformations of Cold-Compressed Multiwalled Boron Nitride Nanotubes Probed by Infrared Spectroscopy *J. Phys. Chem. C* **114** 1782–8

[51] Lim S H, Luo J, Ji W and Lin J 2007 Synthesis of boron nitride nanotubes and its hydrogen uptake *Catalysis Today* **120** 346–50

[52] Geick R, Perry C H and Rupprecht G 1966 Normal Modes in Hexagonal Boron Nitride *Phys. Rev.* **146** 543–7

[53] Ferreira T H, Hollanda L M, Lancellotti M and de Sousa E M B 2015 Boron nitride nanotubes chemically functionalized with glycol chitosan for gene transfection in eukaryotic cell lines *Journal of Biomedical Materials Research Part A* **103** 2176–85

[54] Fu C, Li Q, Lu J, Mateti S, Cai Q, Zeng X, Du G, Sun R, Chen Y, Xu J and Wong C-P 2018 Improving thermal conductivity of polymer composites by reducing interfacial thermal resistance between boron nitride nanotubes *Composites Science and Technology* **165** 322–30

[55] Bai Y, Wang L, Ge C, Liu R, Guan H and Zhang X 2020 Atomically thin hydroxylation boron nitride nanosheets for excellent water-based lubricant additives *Journal of the American Ceramic Society* **103** 6951–60

[56] Guo Y, Ruan K, Shi X, Yang X and Gu J 2020 Factors affecting thermal conductivities of the polymers and polymer composites: A review *Composites Science and Technology* **193** 108134

[57] Chang E, Ameli A, Alian A R, Mark L H, Yu K, Wang S and Park C B 2021 Percolation mechanism and effective conductivity of mechanically deformed 3-dimensional composite networks: Computational modeling and experimental verification *Composites Part B: Engineering* **207** 108552

[58] Yu C, Gong W, Tian W, Zhang Q, Xu Y, Lin Z, Hu M, Fan X and Yao Y 2018 Hot-pressing induced alignment of boron nitride in polyurethane for composite films with thermal conductivity over 50 Wm−1K−1 *Composites Science and Technology* **160** 199–207

[59] Ding P, Zhang J, Song N, Tang S, Liu Y and Shi L 2015 Anisotropic thermal conductive properties of hot-pressed polystyrene/graphene composites in the through-plane and in-plane directions *Composites Science and Technology* **109** 25–31